Published in Inflammation Research 7, issue 3, 411-420, 1977
which should be used for any reference to this work

Adsorption and Structural Studies on Activated Carbons[1]

By H.F. STOECKLI and U. HUBER
Institut de Chimie de l'Université, Avenue de Bellevaux 51, CH-2000 Neuchâtel, and Gruppe für Rüstungsdienste, TA 8, AC-Laboratorium, CH-3752 Wimmis, Switzerland

Abstract

The porous structure of activated carbons is examined from the point of view of gas adsorption, and in relation to classical methods such as X-ray diffraction and electron microscopy. It is suggested that the different approaches to the problem of microporosity should provide complementary information, which can be useful for a better understanding of static and dynamic adsorption processes in activated carbons.

Introduction

Owing to their high adsorption capacity, activated carbons [1] have found a wide range of applications in processes such as the purification of gases, the separation of various mixtures and the recovery of solvents, for example. There exists a direct relation between the adsorptive properties of these materials and their texture, which consists mainly of cavities of molecular dimensions called micropores. The widths of these cavities are typically found in the region of 0.5 to 0.8 nm, and in some cases they do not exceed 0.5 nm. This gives the material typical molecular-sieve properties [2]. Factors like the size and shape of the micropores, as well as their distribution, are therefore of fundamental importance in the understanding and the assessment of adsorptive properties. In this context, the present contribution is a short survey describing possible methods for structural studies on activated carbons, in relation to their adsorption properties. Typical examples from routine investigations on series of carbons will be used to illustrate the methods. It will also be shown that the different types of investigation lead to a consistent pattern for the microporous structure of active carbons.

[1]) Dedicated to K. Bucher on the occasion of his 65th birthday.

Origin and manufacture of active carbons

Active carbons can be produced practically from any carbonaceous raw material, but economical factors reduce the choice. Industrial production is usually based on wood (saw dust, fruit stones, nutshells), coke and coal, but there is a growing interest in wastes such as lignin (sulphite liquor) and residues from the petroleum industry. In the case of carbons with molecular-sieve properties, organic polymers are the common starting material.

Technically, active carbons are prepared either by a two-step or a single-step procedure, as shown below

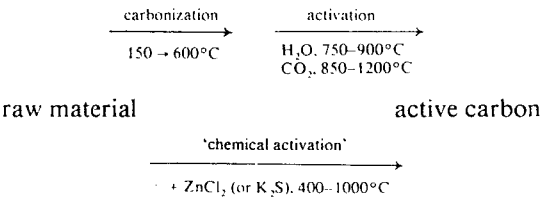

In the first method, one begins with a carbonization stage, during which most of the non-carbon elements (H and O) are removed and the freed atoms of elementary carbon form graphitic sheets of very small dimensions. Simultaneously, tarry substances are formed. During the following step, called 'physical' activation, the pore system is developed by the removal of the tarry material. This is obtained by the reaction with steam or carbon dioxide at high temperatures. The degree of activation is characterized by the so-called burn-off, which represents the percentage of weight loss during the operation.

In the second method, active carbon is prepared in a single step, by adding to the raw material substances like $ZnCl_2$ or K_2S. These compounds prevent the formation of tarry substances on a large scale. This method is usually called 'chemical' activation, although improperly. The resulting material can also be submitted to a further treatment with steam or carbon dioxide, in order to develop the pore system.

It is well known, that the conditions under which activation is carried out can have a strong influence on the properties of the final product, and it has recently become possible to obtain carbons with molecular-sieve properties, by starting with coal instead of polymers [3].

The porosity of activated carbons in general

As mentioned above, activated carbons owe their specific adsorption properties to the existence of a very fine pore system, although a wide range of pore sizes may be present in the material. The larger pores are of great importance in the transport of matter from the liquid or the gas phase into the fine pores. It is therefore of interest to investigate the whole range of porosity of such solids.

For reasons of experimental convenience, pores are divided into three classes which are [4]

(a) macropores, with widths exceeding 50 nm (500 Å)
(b) mesopores, covering the range of 2–50 nm, and
(c) micropores, having widths of less than 2 nm.

This definition is based on the fact that capillary condensation can occur in pores having radii or widths of more than 1.5 to 2 nm, when condensable gases are adsorbed. By using well-known experimental techniques and the equation of Kelvin [5], it is possible to characterize effectively the range of porosity (b). Macroporosity and the major part of mesoporosity can be investigated by mercury porosimetry [6], which covers approximately the range of 5–7500 nm, depending on the experimental conditions. This method is based on the relation which exists between the external pressure p and the radius r_p of the smallest pores being filled by mercury,

$$r_p = (2\gamma/p)\cos\phi \qquad (1)$$

For mercury at 293 K, $\gamma = 480$ dyn/cm and $\phi = 140°$ [5]. Figure 1 shows the variation of the pore volume V_p as a function of r_p, for typical

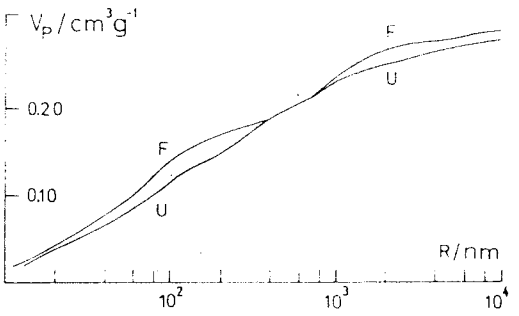

Figure 1
Mercury porosimetry diagram for activated carbons of series F and U.

activated carbons of series F and U (vegetable and mineral origin). The slope of the curve characterizes the relative importance of the different pore sizes in the material. In the present examples, the distributions are almost uniform in the range of 10 to 1200 nm, and decrease rapidly at higher values. The total volume of the pores larger than 7.5 nm is close to 0.30 cm^3/g in both cases.

Information about the pores in the range of 2–7.5 nm can be obtained from the interpretation of the adsorption hysteresis which is caused by capillary condensation in the mesopores. Experiments are usually carried out with N_2 at 77 K, or with other simple gases adsorbed near their normal boiling point temperature. Since this technique covers the range of 2–50 nm, there is an interesting overlap with mercury porosimetry, providing a check for consistency [6]. In the case of carbon U, for example, it is found that there exists a significant mesoporosity in the range of 2.5 to 4.5 nm, which amounts to 0.45 cm^3/g. Samples of the F series, on the other hand, show no mesoporosity and one may conclude that the micropores are directly accessible from large pores. Such differences illustrate the influence of the activation process on the structure of the final material.

Microporosity can be assessed either by careful density measurements in liquids such as benzene, which are compared with the densities in mercury, or better by direct adsorption measurements from the gas phase [1, 2, 5]. The latter technique is the most reliable and it yields values of the total micropore volume, as seen by the different probes. The interpretation of the adsorption experiments is based on the equation of Dubinin and Radushkevich, described in a following section.

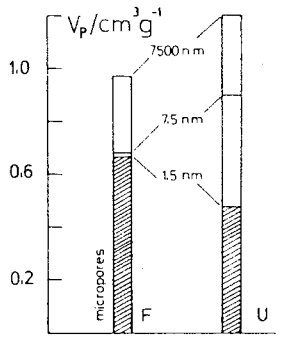

Figure 2
The distribution of porosity in activated carbons F and U.

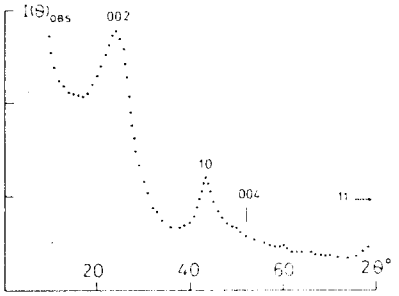

Figure 3
X-ray powder diffractogram for carbon U.

The combination of the different results can be used to characterize the relative importance of the three types of porosity in active carbons, as shown in Figure 2. This diagram illustrates the effect of the precursor material and the activation. This type of representation is also useful in the study of increasing activation on a given carbon.

Since the specific properties of activated carbons depend essentially on the micropores, it is desirable to refine the description of this type of porosity. In the line of the foregoing method, an assessment of the lower micropore region (< 0.7 nm, approximately) can be obtained from molecular-sieve experiments with probes of increasing molecular dimensions [2, 7–9]. Such studies involve the use of molecules like helium (0.25 nm), nitrogen (0.30 nm), benzene (0.34 × 0.68 nm), carbon tetrachloride (0.69 nm) and α-pinene (0.69 to 0.80 nm), for example. It was found [7] that in a carbon based on the co-polymer 'Saran', neopentane (0.62 nm) was only adsorbed to 10% of the value of benzene, which suggests the existence of slit-shaped micropores. On the other hand, in the case of strongly activated carbons, the selectivity disappears gradually, which indicates a shift towards larger micropores. It is obvious that such differences in the micropore structure are of great importance in the choice of activated carbons for specific purposes.

Estimates for the size and shape of typical micropores can also be obtained from adsorption energies, which are derived from a thermodynamic treatment of adsorption data [10]. Typical results obtained from gas-solid chromatography experiments with simple molecules on carbon columns, indicate that the interaction energies are approximately 1.7 times larger in micropores than on a single flat surface of the same nature (graphitized carbon blacks) [10, 11]. The enhancement of the adsorption energy is caused by the small dimensions of the micropores, in which the force fields of opposite walls can overlap. Theoretical calculations can be carried out for simple models, a plausible one being that of slit-shaped micropores. This model is suggested by experiments of the type described above, and by the study of absorption kinetics, where it is found that flat molecules like benzene are adsorbed faster than globular ones [12]. Another argument in favour of parallel-walled micropores is the presence of small graphitic sheets in activated carbons, as revealed by X-ray and electron microscopy studies (see following section). The corresponding theoretical treatments [10, 11] suggest pore-widths in the region of 0.6–0.8 nm, in agreement with independent determinations [2, 7–9].

Structural studies by X-rays and electron microscopy

Like other carbonaceous materials, activated carbons can be investigated by X-ray analysis at small and wide angles, within a standard theoretical framework [13, 14]. This type of study provides information of a statistical nature, since it is based on the interaction of a large amount of matter with the X-rays.

The typical powder diffractogram shown in Figure 3 corresponds to sample U in the range $10° < 2\theta < 80°$. The principal characteristic, with respect to a well-organized material like graphite, is the presence of a diffuse (002) reflexion and of (*hk*) bands such as (10) and (11), instead of the general (*hkl*) reflexions. As shown first by WARREN [15], such a pattern corresponds

to the random (or turbostratic) stacking of a limited number of small graphitic sheets. These are characteristic for a wide variety of paracrystalline or so-called 'amorphous' carbons [14].

After correction for various effects (instrumental factors, absorption, polarization, incoherent scattering), the observed intensities can be submitted to theoretical treatment [14, 16, 17]. The broadening of the peaks is commonly used to derive structural parameters of the turbostratic stacks. The height of the stacks, L_c, can be calculated from the (002) or any other (00l) reflexion by using the equation of Scherrer [14, 15]

$$L_c = 0.94\lambda/B_{(00l)} \cos\theta \qquad (2)$$

where $B_{(00l)}$ is the peak breadth at half the maximum intensity. It has been pointed out, that the value of the constant (0.94) becomes a function of the size, in the case of small stacks [14, 16], and since the broadening of a (00l) reflexion can also be caused simultaneously by the size of the particle and imperfections in the stacking [18], L_c must be treated with care.

The quantity L_a, which should represent the average diameter of the graphitic sheets, is given by the equation of WARREN [14, 15]

$$L_a = 1.84\lambda/B_{(hk)} \cos\theta \qquad (3)$$

where $B_{(hk)}$ represents the width of the (11) and (10) bands. However, as pointed out by WARREN himself [16], reliable values can only be obtained if $L_a > 5$ nm. This means that in the case of activated carbons, where $L_a \simeq 1$–2 nm and $L_c \simeq 1$ nm (two or three sheets), more refined treatments are required in order to obtain reliable parameters. The need for a more accurate description is also suggested by inconsistencies which are frequently found when observations are simultaneously carried out in high resolution microscopy [18].

Another useful source of information is the scattering of X-rays at small angles [13, 14, 19, 20]. It arises from heterogeneities in solid matrices, which are the pores in the case of activated carbons. Depending on the situation, various quantities can be derived from the scattering curve. The most easily available are:

(a) The so-called gyration radius R_g, introduced by GUINIER [13], which is a shape-dependent pore dimension. It is obtained from a plot of $I(s)$ against s^2, where $s = \sin 2\theta/\lambda$. A careful analysis shows that the theory of Guinier strictly applies to the case of dilute pore systems in the solid (small to average degree of activation). Deviations from linearity in the case of a significant porosity must therefore be interpreted carefully. For sample U, for example, the absence of linearity must rather be ascribed to the high micro and mesoporosity (Fig. 2), than to the effect of the heterogeneity in the micropore system. The gyration radius R_g has been determined by DUBININ and PLAVNIK [21] for active carbons with a smaller, but still significant degree of activation. Typical values of R_g were in the range of 0.5 to 0.8 nm. For micropores having the shape of disks [22], these values would also correspond to the widths (height of the disks), if the diameter is approximately 2 nm. This is a plausible model, in agreement with the calculations from adsorption energies [10, 11] quoted above. In certain cases, Dubinin and Plavnik also found values of R_g in the range of 1.1–1.5 nm, which corresponds to larger micropores (supermicropores). These have also been observed in adsorption experiments [23], as discussed in the following section.

(b) The correlation distance a [19], introduced by DEBYE [24], is not limited to dilute systems like R_g. It can be shown that for randomly distributed pores, the scattered intensity curve is given by

$$I(\theta) = A/[1 + (4\pi\theta a/\lambda)^2]^2. \qquad (4)$$

This means that a can be obtained from a plot of $I(\theta)^{-1/2}$ against θ^2 (Fig. 4). The quantity a is related to l_p and l_m, the average lengths of all the segments in the pores and in matter, by

$$l_p = a/(1 - P) \quad \text{and} \quad l_m = a/P \qquad (5)$$

where P is the volumic fraction of the pores in the solid. For carbons like the examples U and F, it is found that l_p is respectively 0.9 and 0.7 nm, which is in agreement with other observations for carbonaceous materials [19, 20].

Since the quantities R_g and l_p both depend on the size and on the shape of the pores [22], their comparison should provide useful information. This possibility has not been fully exploited yet, but it is certain that the results should be compatible with the molecular-sieve experiments [2, 7–9] described in the previous section.

Owing to its fast development in the past years, transmission electron microscopy (TEM) has become a useful tool for structural investigations of carbonaceous materials [25, 26]. The main advantage of this method over X-ray

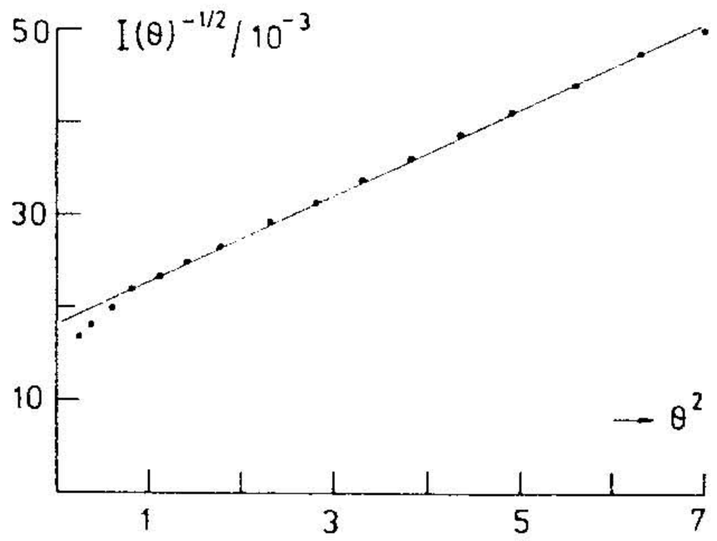

Figure 4
Typical Debye plot for a carbon of series U.

analysis, is the possibility of a choice within the samples under investigation. As shown by OBERLIN and coworkers [26], very fine details can be observed unambiguously when the lattice imaging and dark-field techniques are used simultaneously at very high resolution. These authors were able to determine directly the dimensions of individual stacks of graphitic sheets for soft carbons and for raw anthracites, for example.

In the case of anthracites, which are possible precursors for activated carbons [1], it was found that the number of layers in a stack was only 2 or 3, with a diameter close to 1.0 nm. Simultaneously, the evolution of the mesoporosity in the range of 3–6 nm could be observed as a function of heat treatment at high temperatures, since these pores appear as clear areas between sinuous dark lines (ribbons of stacks). Although the direct observation of micropores is not yet possible, the full use of TEM techniques should significantly promote our knowledge of the fine structure of activated carbons. As examples, typical micrographs are shown in Figures 5–7. They correspond to the same sample of activated carbon U, at various magnifications. Figure 5 shows the general morphology of a granule at low magnification (Stereoscan). Figures 6 and 7 correspond to thin regions observed in TEM at high resolution. It can be seen that activation is not homogeneous and the limiting case of burning out (edge of a thin particle) is shown in Figure 7.

Adsorption of gases in micropores

Finally, we shall consider the adsorption properties of activated carbons, which can be understood in the light of the preceding sections.

Molecules from the gas phase will interact with the solid and, as a result, adsorption will take place on the open surface and in the micropores. As mentioned earlier, the energy of adsorption is stronger in the micropores and therefore the molecules will fill these pores first and reversibly (no capillary condensation can occur, as mentioned earlier). Some problems may arise, however, if constrictions are present in the pore system [2]. The process of micropore filling is described by the theory of DUBININ [1, 27], which has been elaborated in successive stages. The fundamental equation, known as the equation of Dubinin and Radushkevich (D–R), is

$$W = W_0 \exp\left[-B(T/\beta)^2 \log^2(p_0/p)\right] \qquad (6)$$

Figure 5
Surface of a typical granule of carbon U at a magnification of 10,000× (courtesy of LSRH, Neuchâtel).

Figure 6
High resolution electron micrograph of carbon U. Final magnification of 1,500,000× (Philips EM-300, underfocussed 80 nm approximately).

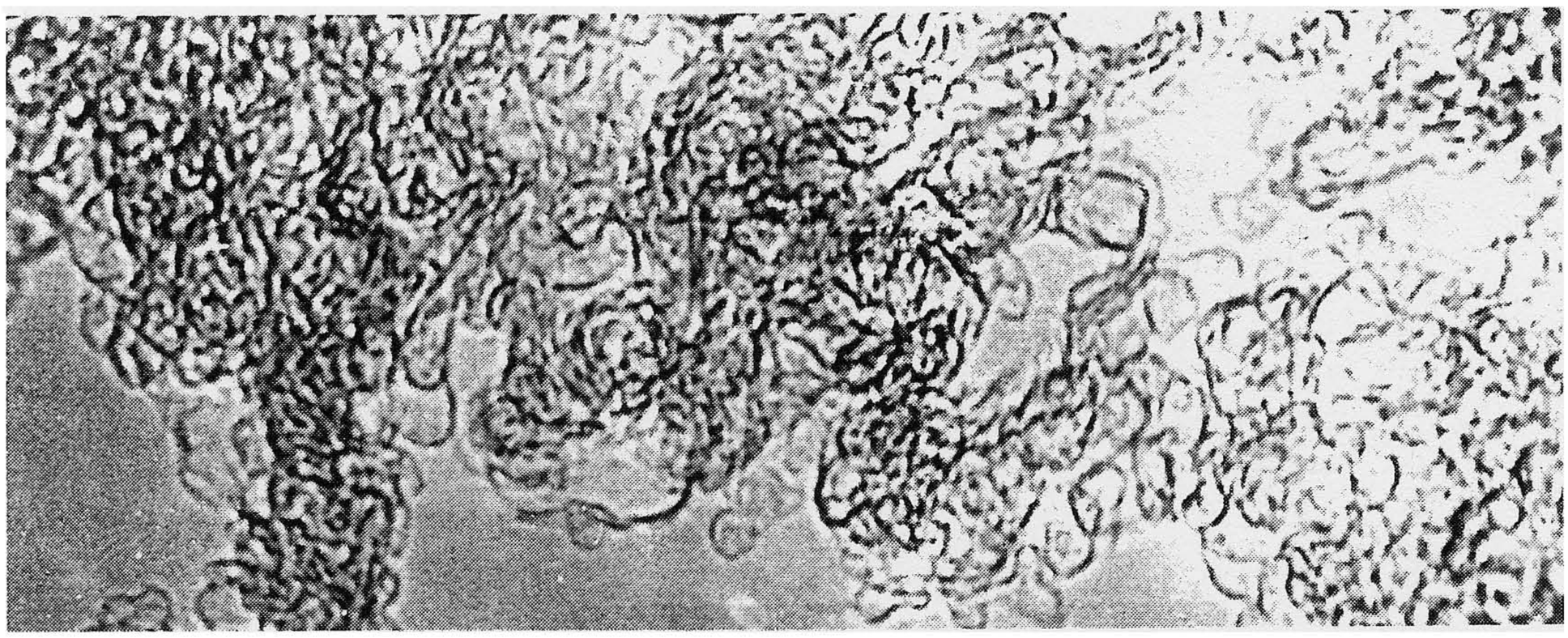

Figure 7
High resolution electron micrograph showing a strongly activated edge (same sample as in Fig. 6). Final magnification of 2,100,000×.

where W is the volume of the liquid-like adsorbate filling the micropores at pressure p and temperature T, W_0 is the total volume of the micropores, and B and β are constants characterizing the solid and the adsorbate. p_0 is the saturation pressure of the gas at temperature T.

For carbons of the F and U series, W_0 varies between 0.45 and 0.80 cm^3/g and B is close to $1.0 \cdot 10^{-6}$.

The main interest of this equation lies in the possibility of predicting to some extent the adsorption of simple gases on a given material, through the knowledge of B and β. Assuming that B, the so-called structural constant, depended only on the solid, Dubinin and his co-workers [1, 27] showed that the similarity or affinity coefficients β had ratios close or equal to the ratios of the Sugden increments (parachores) of the adsorbates. Benzene was chosen as a reference and consequently $\beta(C_6H_6) = 1.0$. Coherent results were obtained by the Soviet school for the adsorption of simple and mostly non-polar substances on various carbons. Although the survey includes relatively large molecules, discrepancies are found when the theory is applied to a wider range of molecules,

including polar ones. In many cases, it is also found that the domain of validity of the (D–R) adsorption equation is very limited or almost inexistent within the usual range of $10^{-5} \lesssim p/p_0 \lesssim 0.1$. This is clearly shown by the limited range of linearity in a plot of $\ln W$ against $\log^2(p_0/p)$. Generalizations and extensions of the (D–R) equation (6) had therefore to be considered. DUBININ and IZOTOVA [23] showed that for certain carbons the experimental results could be interpreted by postulating contributions from two different micropore systems to the overall isotherm,

$$W = W_{01} \exp[-B_1(T/\beta)^2 \log^2(p_0/p)] + W_{02} \exp[-B_2(T/\beta)^2 \log^2(p_0/p)] \quad (7)$$

These systems are characterized by their respective volumes, W_{01} and W_{02}, and their structural constants B_1 and B_2. As mentioned in the previous section, Dubinin and Plavnik were able to confirm the existence of two types of micropores, having gyration radii of 0.5–0.8 nm and 1.1–1.5 nm [21, 27]. A comparative analysis of adsorption data and the results from X-rays, as quoted by these authors, suggests the following empirical relation [28]

$$\bar{R}_g = (62 \cdot B \cdot 10^6)^{1/2} \quad (8)$$

This would confirm the existence of a direct relation between the structural constant B of Eq. (6) and the size of the micropores, as postulated by Dubinin over twenty years ago (B generally increases with the degree of activation). It is therefore possible to ascribe a physical meaning to constant B.

More recently, DUBININ and ASTAKHOV [27] have suggested a generalization of the fundamental equation for the filling of micropores, in the form

$$W = W_0 \exp[-(A/E)^n] \quad (9)$$

where $A = RT \ln(p_0/p)$ and E is a specific quantity containing implicitly B and β. The new parameter is the variable exponent n, which can range from 2 to 6 in the case of zeolites. This equation has also been used to describe adsorption by certain activated carbons which do not follow Eq. (6) in a satisfactory way [29], and it was found that n decreases with increasing activation. However, when a large range of temperature and relative pressures is considered [28], the experimental results for adsorption by strongly activated carbons (like series F and U) cannot be fully represented by the Dubinin–Astakhov Eq. (9). It was therefore suggested by STOECKLI [30], that one should rather use an extended form of Eq. (7),

$$W = \sum W_{0j} \exp[-B_j(T/\beta)^2 \log^2(p_0/p)] \quad (10)$$

The overall isotherm is therefore the result of a weighted contribution from the different types of micropores present in the material. If one assumes a smooth distribution of W_{0j} with B_j, Eq. (10) can be replaced by an integral

$$W = \int_0^\infty f(B) \exp[-B \cdot y] dB \quad (11)$$

where

$$y = (T/\beta)^2 \log^2(p_0/p) \quad (12)$$

For a normalized Gaussian distribution

$$f(B) = (W_0/\Delta\sqrt{2\pi}) \exp[-(B - B_0)^2/2\Delta^2] \quad (13)$$

the integral transform (11) becomes

$$W = W_0 \exp[-B_0 \cdot y] \cdot \exp[y^2\Delta^2/2] \cdot [1 - \mathrm{erf}(x)]/2 \quad (14)$$

The quantity $x = (y - B_0/\Delta^2)\Delta/\sqrt{2}$, and $\mathrm{erf}(x)$ is the tabulated error function.

This adsorption isotherm is more flexible than (10) and it should provide better means for the description of adsorption by heterogeneous carbons. The analysis of experimental results obtained with simple gases on carbons of the F and U series shows that each solid is characterized by specific values of W_0, B_0 and Δ. It is also found that Δ, the spread of B around the maximum B_0 of the distribution, varies with the degree of activation. In some cases, it can be as high as $0.3 \cdot 10^{-6}$, compared with $B_0 \simeq 1.0 \cdot 10^{-6}$.

As an example, Figure 8 shows the variation of $\ln W$ with the quantity $y = (T/\beta)^2 \log^2(p_0/p)$, in the case of carbon F (Fig. 2, for the porosity distribution). It can be seen that the experimental points for the different gases (N_2, Xe, SF_6 and N_2O) fall on the same curve. The linear part of the graph, near the origin, corresponds to the region where the filling of the micropores can be approximated by the (D–R) Eq. (6). The type of curvature shown in Figure 8 has been observed by different authors [29]. It can be described by the Dubinin–Astakhov Eq. (9) only for the range of $y < 4 \cdot 10^6$ in the present case. As shown in Figure 9, it was also found that carbons with strong molecular-sieve properties follow closely

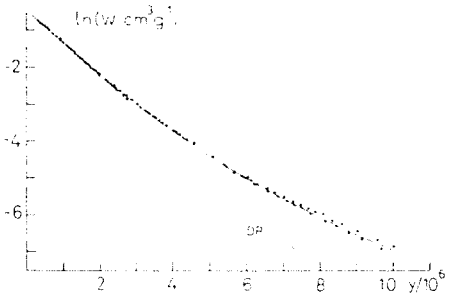

Figure 8
Representation of $\ln W$ against $y = (T/\beta)^2 \log^2(p_v/p)$ in the case of a carbon of the F series. The overall temperature range is 78 to 320 K.

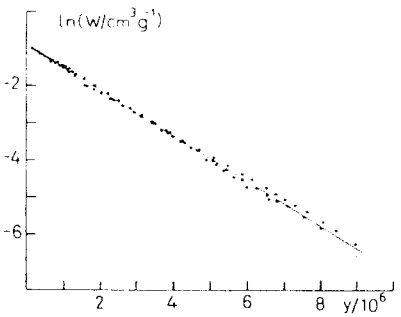

Figure 9
Adsorption by a polymer-based carbon with molecular-sieve properties. The experimental conditions are the same as in Figure 8.

the (D–R) equation, under the same experimental conditions as in the case of sample F. This observation supports the basic idea of the generalization of Eq. (6), leading to (10) and (14).

The advantage of Eq. (14) over (9) is the fact that a physical meaning can be ascribed to the parameters B_0 and Δ, through the empirical expression (8). In the last analysis, it means that information about the micropore system could also be derived from extended adsorption measurements, and it is obvious that the results must be compatible with those of methods of the type described in the previous sections.

The importance of the pore sizes and their accessibility becomes obvious when one considers the adsorption of gases from a stream [1, 31–33]. This corresponds to the situation in which activated carbons are effectively used for technological applications (gas purification, solvent recovery, separation of mixtures). Under such circumstances, the problems of convective mass and heat transfer have to be considered in addition to the problem of adsorption equilibrium and kinetics of mass transport in a porous medium.

For the adsorption of a single component from a gas stream, the following equation can be used for the mass balance,

$$v_l \left(\frac{\partial c}{\partial x}\right)_t = \rho_b \left(\frac{\partial n}{\partial t}\right)_x + \varepsilon \left(\frac{\partial c}{\partial t}\right)_x \qquad (15)$$

(the symbols are listed at the end of the section).

Convective mass transport appears in the left-hand side of Eq. (15), and the kinetics of mass transfer are dealt with in the right-hand side. The concentrations n and c are also related through the adsorption isotherm.

In the case of adsorption from the gas phase, the following steps have to be considered

(a) free diffusion to the external surface of the granules and into macropores,
(b) capillary diffusion in narrow macropores, and
(c) surface diffusion in meso and micropores.

These steps depend on the adsorption isotherm and on factors such as the concentration and the molecular dimensions of the adsorbate, the pore size distribution in the solid, the flow rate of the carrier gas, and the temperature. The influence of these various factors can be analysed by performing numerical simulations of the adsorption process, and by comparing the results with the experimental breakthrough curves for given systems. These computations are based on a clear choice of assumptions [33] as to the various elementary processes which appear in the mass balance equation. At this stage, the knowledge of the system under investigation is of great importance.

Since the concentration gradient in the system is the driving force of the mass transfer, the shape of the adsorption isotherm has a great influence on the breakthrough curve. In the case of type I isotherms [5, 32], like the (D–R) equation discussed above, there exists a relatively short zone in the adsorption bed, over which the concentration in the gas phase falls from the initial value c_0 to zero [32]. This front travels with a uniform speed through the system and it manifests itself in the form of an S-shaped breakthrough curve at the exit. The breakthrough time t_b, at which a certain predetermined concentration appears, sets the limit for the service time of the adsorbent bed under the given

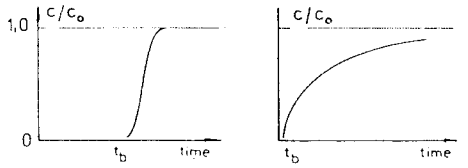

Figure 10
Schematic representation of breakthrough curves for active carbon beds [34] in the case of type I and type III adsorption isotherms (left and right, respectively).

conditions. In the case of type III isotherms, like water in activated carbons, the breakthrough time is almost zero [34]. This is a consequence of the poor adsorption of water at small relative pressures.

The two cases are shown in Figure 10.

Since the adsorption front travels at a constant velocity, there exists a linear relation between t_b and the length of the active carbon bed or the amount of adsorbent. This is given by the well-known equation of Mecklenburg [35],

$$t_b = An_0(x-h)/c_0\dot{V} \qquad (16)$$

(symbols defined at the end of the section).

Similar equations have also been used by different authors [36], in which empirical rate constants are used. In view of the empirical character of these quantities, it follows that such expressions are only valid for specific systems, and under well-defined conditions. Consequently, generalizations are difficult or impossible, and this approach becomes useless if one considers more than one component at a time, or if the flow rate, the concentration c_0, and the temperature of the bed vary with time. The same is also true for the methods which are based either on the concept of equivalent theoretical plates, or on heights of transfer units (HTU) [37].

The general problem of dynamic adsorption can therefore only be dealt with efficiently if one considers numerical simulations. This is a direct procedure, based on a mass balance equation like (15), involving several parameters, and requiring a large amount of computing. The choice of the assumptions regarding the various processes is based on the following type of information:

- the adsorbent (porosity in general, specific parameters for the adsorption isotherm)
- the adsorbate (physical properties and specific parameters for the isotherm)
- the geometry of the adsorbent bed (size of the granules, packing density)
- the dynamic characteristics (flow rate and concentrations)
- the temperature and the thermal conductivity in the system.

The study of one-component systems has shown that the exact knowledge of the adsorbent and of the adsorption mechanism are of decisive importance in the prediction of the breakthrough curves. The analysis of a number of results also suggests the possibility of separating the intrinsic characteristics of the adsorption bed from the specific adsorbent–adsorbate interaction parameters. Satisfactory results have already been obtained in the computation of breakthrough curves for simple systems.

List of symbols not defined in the text.

- A cross-section of the bed (cm^2)
- c concentration of the adsorbate in the gas (g/cm^3)
- c_0 initial concentration
- h critical bed length (cm)
- n concentration of the adsorbate in the adsorbent (g/g)
- n_0 value of n in equilibrium with c_0 (g/cm^3)
- $\dot{V}$ volume flow rate (cm^3/s)
- v_l linear velocity (cm/s)
- x length of the bed (cm)
- ε interparticle volume (cm^3/cm^3)
- ρ_b bulk density of the packed bed

Acknowledgments

The authors wish to thank Messrs. A. Perret and J. Ph. Houriet (Neuchâtel) for providing unpublished results, and Dr. J. Dubochet (Biozentrum Basel) for the optical transforms of our EM micrographs.

Received 21 June 1977.

References

[1] M. Smizek and S. Cerny, *Active Carbons* (Elsevier, Amsterdam, 1970).
[2] P.L. Walker, Jr., L.G. Austin and S.P. Nandi, *Chemistry and Physics of Carbon*, vol. 2 (Marcel Dekker, New York, 1966).
[3] H. Juentgen, International Carbon Conference, Baden-Baden, 1976.
[4] D.H. Everett, *Definitions, Terminology and Symbols in Colloid and Surface Chemistry*, Pure appl. Chem. *31*, 585 (1972).
[5] J.S. Gregg and K.S.W. Sing, *Adsorption, Surface Area and Porosity* (Academic Press, London, 1967).
[6] A. Guyer, Jr., B. Boehlen and A. Guyer, Helv. Chim. Acta *42*, 2103 (1959). E. Barrett, L. Joyner and P. Halenda, J. Amer. Chem. Soc. *73*, 3155 (1951).
[7] L.B. Adams, E.A. Boucher and D.H. Everett, Carbon *8*, 761 (1970).

[8] A.N. AINSCOUGH, D. DOLLIMORE and G.R. HEAL, Carbon *11*, 189 (1973). H. MARSH and H.G. CAMPBELL, Ibid. *9*, 489 (1971).
[9] E. FITZER and J. KALKA, Carbon *10*, 173 (1972).
[10] D.H. EVERETT and J.C. POWL, J.C.S. Faraday Trans. *I*, 1976, 619.
[11] H.F. STOECKLI, Helv. Chim. Acta *57*, 2192 (1974). H.F. STOECKLI and A. PERRET, Ibid. *58*, 2318 (1975).
[12] J.R. DACEY and D.G. THOMAS, Trans. Faraday Soc. *50*, 740 (1954).
[13] A. GUINIER and G. FOURNET, *Small Angle Scattering of X-rays* (John Wiley, New York, 1955). W.W. BEEMANN, P. KAESBERG, J. ANDEREGG and M.B. WEBB, *Handbuch der Physik*, vol. 32 (Springer, Berlin, 1957). A. GUINIER, *Théorie et Technique de la Radiocristallographie*, (Dunod, Paris, 1964).
[14] S. ERGUN, *Chemistry and Physics of Carbon*, vol. 3 (Marcel Dekker, New York, 1968). W. RULAND, ibid., vol. 4 (1968). J.C. BOKROS, ibid., vol. 5 (1969).
[15] B.E. WARREN, Phys. Rev. *59*, 693 (1941). J. BISCOE and B.E. WARREN, J. Appl. Phys. *13*, 364 (1942).
[16] B.E. WARREN and P. BODENSTEIN, Acta Cryst. *18*, 282 (1965); *20*, 602 (1966).
[17] R.R. SCHEEL and R.A. FRIEDEL, *X-ray Studies of the Structure of Cokes Carbonized at Different Temperatures*, Report of Investigation No. 7883 (U.S. Dept of the Interior, Bureau of Mines, 1974). S. ERGUN, Carbon *14*, 139 (1976). F. ROUSSEAUX and D. TCHOUBAR, Carbon *15*, 55 (1977).
[18] S. ERGUN, Phys. Rev. *B1*, 3371 (1970).
[19] G.D. WIGNALL and C.J. PINGS, Carbon *12*, 51 (1974).
[20] R.G. JENKINS and P.L. WALKER, Carbon *14*, 7 (1976).
[21] M.M. DUBININ and G.M. PLAVNIK, Carbon *6*, 183 (1968). G.M. PLAVNIK and M.M. DUBININ, Izv. Akad. Nauk SSSR (ser. Khim.) 1966, 628.
[22] *International Tables for X-ray Crystallography*, vol. III (The Kynoch Press, Birmingham, 1968), pp. 324–329.
[23] T.I. IZOTOVA and M.M. DUBININ, Zh. Fiz. Khim. *39*, 2796 (1965).
[24] P. DEBYE and A.M. BUECHE, J. Appl. Phys. *20*, 518 (1949). P. DEBYE, H.R. ANDERSON and H. BRUMBERGER, ibid. *28*, 679 (1957).
[25] E.L. EVANS, J.L. JENKINS and J.M. THOMAS, Carbon *10*, 637 (1972). J.L. KAE, Ibid. *13*, 55, 246 (1975). D.J. JOHNSON, I. TOMIZUKA and O. WATANABE, Ibid. *13*, 321 (1975). A. OBERLIN, M. OBERLIN and M. MAUBOIS, Phil. Mag. *32*, 833 (1975).
[26] A. OBERLIN and G. TERRIERE, C.R. Acad. Sci. Paris *C275*, 649 (1972). A. OBERLIN, G. TERRIERE and J.L. BOULMIER, Tanso *80*, 29 (1975). A. OBERLIN and G. TERRIERE, Carbon *13*, 367 (1975).
[27] M.M. DUBININ, *Progress in Surface and Membrane Science*, vol. 9 (Academic Press, New York, 1975). M.M. DUBININ, *Chemistry and Physics of Carbon*, vol. 2 (Marcel Dekker, New York, 1966).
[28] H.F. STOECKLI and J. PH. HOURIET, Carbon *14*, 253 (1976).
[29] B. RAND, J. Colloid Interface Sci. *56*, 337 (1976).
[30] H.F. STOECKLI, J. Colloid Interface Sci. *59*, 184 (1977).
[31] V. PONIEC, Z. KNOR and S. CERNY, *Adsorption on Solids* (Butterworth, London, 1974).
[32] A.V. KISELEV and Y. YASHIN, *La Chromatographie Gaz-Solide* (Masson, Paris, 1969).
[33] T.W. WEBER and R.K. CHAKRAVORTI, A.I.Ch.E. J. *20*, 228 (1974). I. ZWIEBEL and J.J. SCHNITZER, A.I.Ch.E. Symp. Ser. *69* (134), 18 (1973). F.X. STUART and D.T. CAMP, ibid., p. 33. M.M. DUBININ, I.T. TERASHKO, O. KADLEC, V.I. ULIN, A.M. VOLOSHCHUK and P.P. ZOLOTAREV, Carbon *13*, 193 (1975). E. COSTA NOVELLA, F. OLTRA OLTRA and J.M. BLASCO ARIAS, Anales de Quim. *71*, 213 (1975). R.D. AMMONS, N.A. DOUGHATRY and J.M. SMITH, Ind. Eng. Fundam. *16*, 263 (1977).
[34] U. HUBER, Dissertation ETH Zürich, No. 4934 (1972).
[35] W. MECKLENBURG, Z. Elektrochem. *31*, 488 (1925).
[36] A. GUYER, Jr., B. BOEHLEN and A. GUYER, Helv. Chim. Acta *42*, 2103 (1959). M.R. KAUFMANN, Dissertation ETH Zürich, No. 4701 (1971). A.L. JONAS and J.A. REHRMANN, Carbon *11*, 59 (1973). M.M. DUBININ, P.P. ZOLOTAREV, K.M. NIKOLAEV, N.S. POLYAKOV, L.I. PETROVA and L.V. RADUSHKEVICH, Izv. Akad. Nauk SSSR (ser. Khim.) 1973, 293.
[37] R.E. TREYBAL, *Mass Transfer Operations* (McGraw Hill, New York, 1955).